Table 1. Solubilities of He^3 and He^4 and calculated isotopic fractionation values for distilled water and seawater at various temperatures. Values shown in columns 2 and 3 are the mean of the number of measurements listed in parentheses; ranges shown are ± 1 standard deviation.

Temperature (°C)	Bunsen solubility coefficient × 10^3 He^3	Bunsen solubility coefficient × 10^3 He^4	(α−1) (%)
	Distilled water		
0.60	9.254 ± 0.026 (4)	9.355 ± 0.004 (4)	−1.1
20.11	8.620 ± 0.016 (4)	8.724 ± 0.024 (6)	−1.2
40.14	8.574 ± 0.019 (5)	8.713 ± 0.036 (4)	−1.6
	Seawater, salinity 36.425 per mil		
0.07	7.655 ± 0.012 (4)	7.771 ± 0.025 (5)	−1.5
20.13	7.339 ± 0.009 (4)	7.420 ± 0.029 (4)	−1.1
40.46	7.346 ± 0.028 (4)	7.488 ± 0.015 (4)	−1.9

Since the Bunsen coefficients for He^3 and He^4 both pass through a minimum at around 30°C, an increase in fractionation might be explained by a greater mass dependence in the processes which govern solubility at temperatures above the minimum.

Without enough values of $(\alpha - 1)$ to justify a more complex treatment, the data were fitted to a linear least-squares regression line:

$$(\alpha - 1)\% = (-1.16 \pm 0.18) - (0.011 \pm 0.007)t$$

where t is the temperature in degrees Centigrade and the errors in the constants represent 1 standard deviation. The 0.28 percent standard deviation of the data about the line is in good agreement with the expected value of 0.3 percent. From the error in the second coefficient it is estimated that the existence of a trend in $(\alpha - 1)$ with temperature can be established only at the 80 percent confidence level.

Although the results show that no gross variations in the fractionation factor occur over the salinity and temperature range studied, further experimental work is needed to precisely establish the nature of such variations. At present $(\alpha - 1)$ for distilled water and seawater is best represented as − 1.2 percent ± 0.2 percent at 0°C, with this value becoming more negative by 0.1 percent with each 10°C increase in temperature.

The results show that for helium the Henry's law constant is lower for the heavier isotope than for the lighter isotope. The same effect was found by Klots and Benson (*6*) for isotopes of oxygen and nitrogen, although the difference was only ~ 0.08 percent for both gases. A larger isotope effect would be expected for helium since there is a much larger percentage mass difference between its isotopes and because it is a monatomic gas.

Clark *et al.* (*1*) report that the He^3/He^4 ratio in their one sample of surface ocean water is depleted by 1.8 percent ± 1.1 percent relative to the ratio in air, where the error quoted is ± 1 standard deviation. At the temperature of their sample (18°C), the results reported here predict a fractionation of − 1.4 percent ± 0.2 percent and are therefore in good agreement with their work.

R. F. WEISS

*Scripps Institution of Oceanography,
University of California, San Diego,
La Jolla 92037*

References and Notes

1. W. B. Clarke, M. A. Beg, H. Craig, *Earth Planet. Sci. Lett.* **6**, 213 (1969).
2. L. T. Aldrich and A. O. Nier, *Phys. Rev.* **74**, 1590 (1948).
3. I. N. Tolstikhin, I. L. Kamensky, B. A. Mamyrin, *Geokhimiya* **1969**(2), 201 (1969); B. A. Mamyrin, I. N. Tolstikhin, G. S. Anufriev, I. L. Kamensky, *ibid.* **1969**(5), 595 (1969).
4. M. S. Goryunov and A. L. Kozlov, *Voprosy geokhumii gelienosnykh gazov i usloviia nakopleniia v semnoi kore* (Russian) (State Sci.-Tech. Pub. Co. Oil and Solid Fuel Lit., Lenningrad-Moscow, 1940); R. E. Zartman, G. J. Wasserburg, J. H. Reynolds, *J. Geophys. Res.* **66**, 277 (1961); E. Mazor and G. J. Wasserburg, *Geochim. Cosmochim. Acta* **29**, 443 (1965); B. D. Gunter and B. C. Musgrave, *ibid.* **30**, 1175 (1966).
5. D. D. Eley, *Trans. Faraday Soc.* **35**, 45 (1939).
6. C. E. Klots and B. B. Benson, *J. Chem. Phys.* **38**, 890 (1963).
7. E. Douglas, *J. Phys. Chem.* **68**, 169 (1964); *ibid.* **69**, 2608 (1965).
8. The equilibration chamber was enlarged to contain approximately 10 ml of water, the constant temperature bath was improved, and procedures for degassing water and transferring gas were checked for air contamination by gas chromatography. The results have been corrected for the effect of the dissolution of the gas on the volume of the aqueous phase.
9. The He^3 used was supplied by Monsanto Research and was specified to be > 99.97 percent He with a He^3/He^4 ratio of 10^4. Air Reduction reactor grade He specified to be > 99.99 percent He was used for the He^4 measurements. Aldrich and Nier (*2*) found the He^3/He^4 ratio to be < 10^{-6} in natural gas wells from which cylinder He is obtained. Gas chromatographic checks of the purity of these gases showed ≦ 0.025 percent and ≦ 0.01 percent air contamination for He^3 and He^4, respectively.
10. Supported by NSF grant No. GA 4558 to the Isotope Laboratory of the Scripps Institution of Oceanography. I thank E. Douglas and P. F. Scholander for teaching me the microgasometric technique, B. Hom for assistance with the laboratory work, G. Arrhenius for supplying the He^3 gas, and H. Craig for critical discussion and support of this research.

24 November 1969

Xenon Hexafluoride: Structure of a Cubic Phase at − 80°C

Abstract. *The crystal structure of a cubic phase of composition XeF$_6$ has been determined at −80°C. There are no simple molecules in the complex structure which involves 1008 atoms distributed over 1600 positions per unit cell. Ions of XeF$_5$$^+$ and F$^-$ are associated in tetrameric and hexameric rings of point group symmetries $\bar{4}$ and 32, respectively. The structure contains right- and left-handed conformations of both tetramers and hexamers. The handedness of the tetramers is disordered but the orientation is ordered. The handedness of the hexamers is ordered but the orientation is disordered.*

We here report the structure of a cubic phase of composition XeF$_6$. The properties of material of this composition pose unusual problems in all states of matter, whether gas, liquid, or solid (*1*). The multiplicity of symmetry relations in cubic space groups with their concomitant restrictions on possible spatial distributions suggests that a cubic phase should be the favored subject for study in the exceptional cases where the option is available.

In 1965 the existence of cubic XeF$_6$ was reported (*2*), with the probable space group $F\bar{4}3c$ or $Fm3c$ and $a = 25.34 \pm 0.05$ Å (temperature not specified). We find that well-formed crystals of cubic XeF$_6$ invariably result when capillaries of FEP (fluorinated ethylene propylene copolymer) partly filled with XeF$_6$ are maintained at 18°C for several days. The sodium fluoride complexing method was used to prepare and purify XeF$_6$ (*3*). The FEP capillaries were prefluorinated with XeF$_6$ and heat-sealed after introduction of the specimens. The crystals give increasingly stronger x-ray reflections as the temperature is lowered. A temperature of − 80°C was selected for intensity measurement as a compromise between quality of data and experimental difficulties. Details of the x-ray cryostat will be described elsewhere (*4*).

A crystal with dimensions 1 by 0.5 by 0.2 mm was used to measure 1023 unique reflections extending out to $d^* = 1.4$ Å^{-1}; Mo radiation, a scintillation counter, and the stationary crystal technique with 10-second counts and background counts on both sides of each reflection were used. With the high cubic multiplicity all measurements could be made with settings of high transmission. There were 487 reflections with peak-to-background ratios in

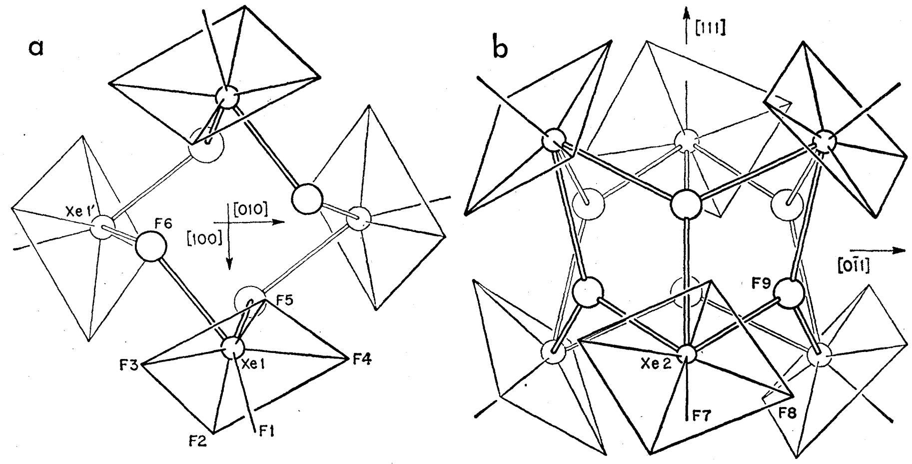

Fig. 1. (a) Tetramer of $XeF_5^+F^-$ centered at 0 0 ¼ with the $\bar{4}$-axis parallel to [001]. Xenon atoms are indicated by small circles and bridging fluoride ions by large circles; XeF_5^+ ions are drawn in skeletal form to preserve clarity. (b) Hexamer of $XeF_5^+F^-$ centered at ¼ ¼ ¼ and oriented with the 3-axis parallel to [111]. The three 2-axes are parallel to $[0\bar{1}1]$, $[10\bar{1}]$, and $[\bar{1}10]$.

excess of three standard deviations in the counting statistics available for analysis. Intensities were corrected for absorption by means of an experimental calibration and for Lorentz-polarization effects. The probable space group was confirmed as $F\bar{4}3c$ or $Fm3c$. The cell constant at − 80°C is 25.06 ± 0.05 Å, which gives a calculated density of 3.73 ± 0.02 g cm^{-3} on the assumption of 144 XeF_6 units per unit cell.

The structure was solved by trial and error. First, spatial and chemical considerations together with key intensity relations were used to locate the 144 xenon atoms. Second, difference syntheses and least-squares refinements were used to locate the 864 fluorine atoms. The fluorine atoms are distributed over 1456 peaks. The analysis with anisotropic thermal parameters for xenon atoms and isotropic thermal parameters for fluorine atoms yields an R factor of 0.070 and a weighted R' factor of 0.052, where

$$R = \frac{\sum |F_o - F_c|}{\sum |F_o|}$$

and

$$R' = \frac{[\sum w(F_o - F_c)^2]^{\frac{1}{2}}}{(\sum wF_o^2)^{\frac{1}{2}}}$$

(the quantities F_o and F_c are the observed and calculated structure factors, respectively, and w is the experimental weight based on counting statistics).

The structure is based on space group $Fm3c$ and contains no distinct molecules. Ions of XeF_5^+ and F^- are associated in tetrameric and hexameric rings of point group symmetries 4 and 32, respectively, as illustrated in Fig. 1, a and b. There are 24 tetramers and eight hexamers per unit cell. The structure contains right-handed and left-handed conformations of both tetramers and hexamers. The enantiomorph of the tetramer (Fig. 1a) is defined by reflection across either a (100) or a (010) plane. Right- and left-handed tetramers are distributed at random. The scattering model contains 24 tetramers of each hand, with an occupancy factor of ½, which superimpose to give 24 configurations of point group symmetry $\bar{4}2m$. The hexamer (Fig. 1b) with its 3-axis parallel to [111] illustrates only one of four orientations which are distributed at random parallel to [111], $[1\bar{1}\bar{1}]$, $[\bar{1}1\bar{1}]$, and $[\bar{1}\bar{1}1]$. The scattering model contains 32 hexamers, with an occupancy factor of ¼, which superimpose to give eight configurations of point group symmetry 432. The enantiomorph of the hexamer (Fig. 1b) is defined by reflection across a $(0\bar{1}1)$, or $(10\bar{1})$, or $(\bar{1}10)$ plane. Right- and left-handed hexamers are distributed in an orderly way. Those of one hand (but with random orientation) occur in configurations centered at ¼ ¼ ¼, ¼ ¾ ¾, ¾ ¼ ¾, and ¾ ¾ ¼. Those of the opposite hand occur in configurations centered at ¾ ¾ ¾, ¾ ¼ ¼, ¼ ¾ ¼, and ¼ ¼ ¾.

There are four structural components in each type of polymer. In the tetramer (Fig. 1a) these are the xenon atom Xe1, the apical fluorine F1, the basal fluorines F2, F3, F4, F5, and the bridging fluorine F6 (*5*). In the XeF_5^+ ion the distances are (estimated standard deviations are given in parentheses) $Xe\text{-}F_{apical} = 1.84(4)$ Å, average $Xe\text{-}F_{basal} = 1.86(3)$ Å, average $F_{apical}\text{-}F_{basal} = 2.29(6)$ Å, and average $F_{basal}\text{-}F_{basal} = 2.54(13)$ Å. The angles are average $F_{apical}\text{-}Xe\text{-}F_{basal} = 77.2$ (1.8)° and average $F_{basal}\text{-}Xe\text{-}F_{basal} =$ 87.2(4.5)°. The bridging F6 has a short contact to Xe1 at 2.23(3) Å, a longer contact to Xe1′ at 2.60(3) Å, and a bridging angle of 120.7(1.2)° at F6. An eight-membered ring results, consisting of four XeF_5^+ ions and four F^- ions with four short and four long bridging contacts. In the hexamer (Fig. 1b) the components are xenon atom Xe2, apical fluorine F7, basal fluorine F8, and bridging fluorine F9. In the XeF_5^+ ion the distances are $Xe\text{-}F_{apical} = 1.76(3)$ Å, $Xe\text{-}F_{basal} = 1.92(2)$ Å, $F_{apical}\text{-}F_{basal} = 2.33(3)$ Å, and $F_{basal}\text{-}F_{basal} = 2.63(3)$ Å, and the angles are $F_{apical}\text{-}Xe\text{-}F_{basal} = 80.0(0.6)$° and $F_{basal}\text{-}Xe\text{-}F_{basal} = 88.3(0.2)$°. The bridging F9 makes equal contacts to three XeF_5^+ ions at 2.56(2) Å with three equal bridging angles of 118.8(0.3)° at F9. A 12-membered ring results, consisting of six XeF_5^+ ions and six F^- ions with 18 equal bridging contacts.

The Gillespie-Nyholm valence-shell electron pair repulsion theory (*6*) clearly finds support in the structure of the XeF_6 cubic phase. A consequence of the theory, recognized by Bartlett in the structures of $[XeF_5]^+[PtF_6]^-$ (*7*) and $XeF_2.IF_5$ (*8*) is that, although an electron pair in the valence shell exerts a larger steric effect than a fluorine ligand, the electron pair is less effective than a fluorine ligand at shielding the positive charge on a xenon or iodine atom. In condensed phases of XeF_6 this poor shielding of the positive charge at the xenon atom has profound consequences. In a free XeF_6 molecule there are always two or three ligands closest to the valence electron lone pair (*9*) that are subject to a maximum repulsive effect. In a condensed phase one or another of these ligands may be expected to be subject to the compound effect of intramolecular electron pair repulsion and intermolecular positive charge attraction. The propensity of XeF_6 for intramolecular rearrangement permits a rapid adjustment toward the tetragonal pyramidal configuration for the XeF_5 fragment of the molecule. Xenon hexafluoride is atypical in all states of matter because of intramolecular rearrangement in the gas phase and association in condensed phases. We believe that both effects can be attributed to the properties of the valence electron lone pair.

R. D. BURBANK
G. R. JONES

Bell Telephone Laboratories, Inc.,
Murray Hill, New Jersey 07974

References and Notes

1. H. H. Hyman, *Science* **145**, 773 (1964); H. Selig, in *Halogen Chemistry*, V. Gutmann, Ed. (Academic Press, New York, 1967), p. 403.
2. P. A. Agron, C. K. Johnson, H. A. Levy, *Inorg. Nucl. Chem. Lett.* **1**, 145 (1965).
3. S. G. Malm, F. Schreiner, D. W. Osborne, *ibid.*, p. 97.
4. R. D. Burbank and S. S. De Bala, in preparation.
5. We use the term "bridging" in the sense of an electrostatic interaction stronger than a van der Waals contact.
6. R. J. Gillespie and R. S. Nyholm, *Quart. Rev. London* **11**, 339 (1957); R. J. Gillespie, *J. Chem. Educ.* **40**, 295 (1963); R. J. Gillespie, in *Noble-Gas Compounds*, H. H. Hyman, Ed. (Univ. of Chicago Press, Chiago, 1963), p. 333; R. J. Gillespie, *Angew. Chem. Int. Ed. Engl.* **6**, 819 (1967).
7. N. Bartlett, F. Einstein, D. F. Stewart, J. Trotter, *J. Chem. Soc.* **1967A**, 1190 (1967).
8. G. R. Jones, R. D. Burbank, N. Bartlett, *Inorg. Chem.*, in press.
9. R. D. Burbank and N. Bartlett, *Chem. Commun.* **1968**, 645 (1968).

9 January 1970

■

Differential Isotopic Fractionation in Benthic Foraminifera and Paleotemperatures Reassessed

Abstract. *Different species of benthic Foraminifera taken at the same level in an Atlantic core yielded different oxygen isotopic values. It was therefore impossible to deduce paleotemperature values. In addition, pelagic and benthic species showed the same isotopic variations, an indication that pelagic and benthic species reflect only the variation of oxygen-18 composition of the ocean.*

During a cruise of the French research vessel *J. Charcot*, the top of Charcot seamount (45°19′N, 10°31′W), which is at a depth of 2665 m and is 2300 m above the Atlantic abyssal plain, was cored.

The core consists throughout its entire length (0.80 m) of calcareous grayish ooze with about 20 percent clays and heavy minerals. The coarse fraction (> 80 μm) is a nearly pure foraminiferal ooze, with pelagic as well as benthic forms. A detailed study of the core has shown that this sediment is Quaternary in age, that it is not reworked, and that the sedimentation rate, obtained by ^{14}C measurements, is about 1.85 cm/1000 years (*1*).

The oxygen isotopic composition of the tests of different foraminiferal species has been studied throughout the core. The pelagic species *Orbulina universa, Globorotalia truncatulinoides,* and *Globorotalia hirsuta,* the benthic species *Planulina wuellestorfi*, a mixture of four species of *Pyrgo* (*myrrhina, depressa, serrata, fisheri*), and a mixture of other calcareous benthic species have been analyzed.

To eliminate the organic matter, the following method proved to be satisfactory (Table 1): (i) grinding the tests; (ii) bathing them for 72 hours in Clorox (sodium hypochlorite) at room temperature; (iii) rinsing four times with deionized water; and (iv) drying at 60°C.

The purified carbonate was then reacted according to McCrea's classical method (*2*). The 8- to 15-mg samples and the 100 percent phosphoric acid were degassed under vacuum for at least 24 hours and were then reacted at 25.2°C in a thermostatic bath while the samples were being continuously shaken. The CO_2 was condensed with liquid nitrogen, released by warming up with a mixture of acetone and Dry Ice, and analyzed with a mass spectrometer, Atlas M 86.

Results are expressed as

$$\delta = \frac{R_{\text{sample}} - R_{\text{standard}}}{R_{\text{standard}}} \times 1000$$

where R is the isotopic ratio $^{18}O/^{16}O$ or $^{13}C/^{12}C$ and the standard is the Chicago PDB-1 standard. All the correction factors mentioned by Craig (*3*) were applied to the results. The reproducibility of the measurements is better than 0.1 per mil.

The results are shown in Fig. 1. It is immediately apparent that the six curves obtained are almost parallel, a group of three curves for the pelagic Foraminifera and a group of three curves for the benthic Foraminifera.

Oxygen isotopic differences among pelagic Foraminifera have been interpreted by Emiliani (*4*) as reflecting the fact that the diverse pelagic species do not live at the same depth and, therefore, not at the same temperature. Evidence from plankton tows equipped with opening and closing nets supports this conclusion (*5*), but the same explanation cannot apply to the benthic species. If the isotopic composition of foraminiferal tests were affected only by temperature and the oxygen isotopic composition of the water, different species of benthic Foraminifera that lived in the same environment would have the same isotopic composition and only one curve would be obtained all along the core for the benthic forms. We obtained, however, three markedly different curves, and the differences between *Pyrgo* sp. and *Planulina wuellestorfi* reached more than 1 per mil.

The same phenomenon has been observed in another core taken on the outer edge of the Atlantic continental shelf, at a depth of 1040 m, 138.6 miles off the Pointe du Raz (47°47′N, 8°06′W). At a level rich enough in benthic forms to allow measurements on separate species, considerable differences in isotopic composition were observed: *Uvigerina mediterranea*, +4.16 per mil; *Cibicides pseudoungerianus*, + 3.40 per mil; *Quinqueloculina* sp. and *Pyrgo* sp., + 3.24 per mil.

In another core, Shackleton (*8*) mentioned a difference of 1.5 per mil between two benthic forms, but he attributed it to a mixture between two levels.

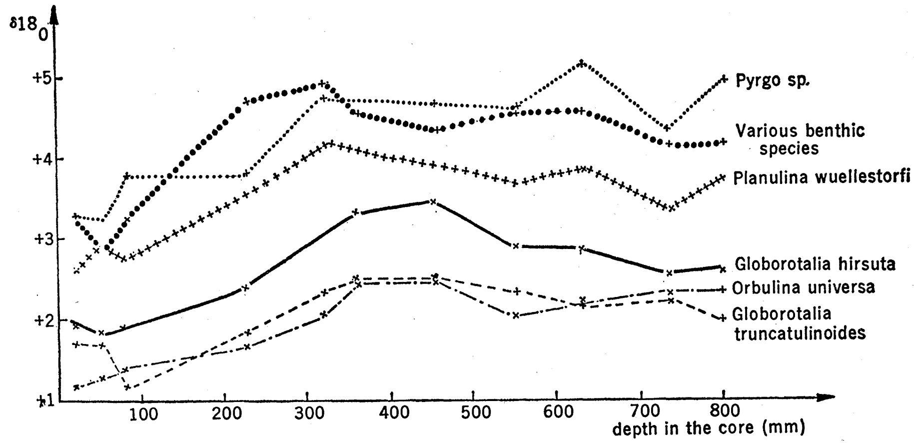

Fig. 1. Variations of $\delta^{18}O$ in three benthic and three pelagic species of Foraminifera in the core.

Tarutani, Clayton, and Mayeda (*7*) have shown that ^{18}O is concentrated in magnesium calcites, relative to pure